Solar cycle variation of network magnetic elements

J. X. Wang* and C. L. Jin

Key Laboratory of Solar Activity of Chinese Academy of Sciences, China
National Astronomical Observatories, Chinese Academy of Sciences, Beijing 100012, China

Abstract. With the unique database from Michelson Doppler Imager aboard the Solar and Heliospheric Observatory in an interval embodying solar cycle 23, the cyclic behavior of solar small-scale magnetic elements is studied. More than 13 million solar network magnetic elements are selected, and the following results are discussed. (1) With increasing flux per element, the number variation of the network elements shows a three-fold scenario: no-correlation, anti-correlation, and correlation with sunspots, respectively. The anti-correlated elements cover flux range of $(2.9 - 32.0) \times 10^{18}$ Mx, and occupy 77.2% of total network elements. (2) The latitude distribution of the correlated elements follows the sunspot butterfly diagram in the solar cycle but has wider latitude distribution than sunspots. Furthermore, the anti-correlated elements also show much broad latitude distribution, but a moderate migration toward equator during the solar maximum which was clearly out of phase with sunspots. These results shed new light in understanding anti-correlated variations of small-scale solar activity, e.g., X-ray coronal bright points, and the origin of the Sun's small-scale magnetism.

Keywords : Sun: activity – Sun: photosphere – sunspots

1. Introduction

The small-scale magnetic fields are observed everywhere on the Sun (Sheeley 1967), i.e., the network fields at the boundaries of super-granulation and intra-network fields (Livingston & Harvey 1975; Smithson 1975) within super-granulation cell. In addition, small-scale emerging bipoles, named ephemeral regions (ERs), which was first described by Harvey & Martin (1973) are observed either on the quiet Sun, or in active regions, with flux from 10^{16} to 10^{20} Mx. The flux emerging rate in ERs exceeds that

---
*email: wangjx@nao.cas.cn

in sunspots by two orders of magnitude (Zirin 1987). A substantial amount of solar magnetic flux is suggested to be still hidden (Trujillo Bueno 2004).

A fundamental question in the solar magnetism is how to understand the origin, dynamics, and cyclic behavior of the small-scale magnetic elements. Do they change in number and flux during a solar cycle and how are they correlated with sunspots? Diverse results on their cyclic variation, e.g., no correlation, anti-correlation and correlation, were reported by either direct magnetic measurements, or indirect observations of small-scale active phenomena (see Jin et al. 2011). The anti-correlation was inferred from cyclic variation of network bright points (Muller & Roudie 1984), HeI 10830 Å dark points (Harvey 1985), coronal X-ray bright points (Davis, Golub & Krieger 1977; Davis 1983; Golub , Davis & Krieger 1979; Sattarov et al. 2010).

Fortunately, the Michelson Doppler Imager aboard the Solar and Heliospheric Observatory (MDI/SOHO) now is providing a unique database, the full-disk magnetograms of more than 13 years covering the complete 23rd Solar Cycle. However, the poor temporal resolution and the sensitivity of the full-disk magnetograms make the identity of ERs and intranet work elements unreliable. Therefore, in this study, we only consider the network magnetic elements.

2. Observations and methods

The details of MDI full-disk magnetograms and data analysis for the study have been described in Jin et al. (2011). In fact, we basically follow the procedures of Hagenaar Schrijver & Title (2003). To have a low noise level, only the 5-min average magnetograms are selected, and a boxcar smoothing function to each magnetogram by a width of $6'' \times 6''$ is applied to reduce the noise. We extract one full-disk magnetogram per day, and thusly select totally 3764 magnetograms from 1996 September to 2010 February. The 23rd solar cycle is covered completely in the data selection and analysis.

The noise level of the smoothed 5-min average magnetograms is about 6 Mxcm^{-2}. We assume that the observed line of sight magnetic flux density is a projection of the intrinsic flux density normal to the solar surface, so the magnetic field is corrected by $B_{cal} = B_{obs}(\alpha)/\cos(\alpha)$, where the angle α is defined by the distance to disk center for each pixel on the disk. We only consider these pixels for which $\alpha \leq 60°$, i.e., the region included by the black circle in the left panel of Fig. 1. For each smoothed and corrected full-disk magnetogram, we apply a magnetic flux density of 15 Mxcm^{-2} as a threshold to define the active regions and their surroundings. The magnetic concentrations with area larger than 9×9 pixels are defined as the active regions (Hagenaar et al. 2003). After excluding the active regions, we apply the magnetic noise, i.e., 6 Mxcm^{-2} as a threshold to create masks for each quiet magnetogram, and define these magnetic islands with more than 10 pixels in size as network magnetic elements (Ha-

Jan 2, 2003
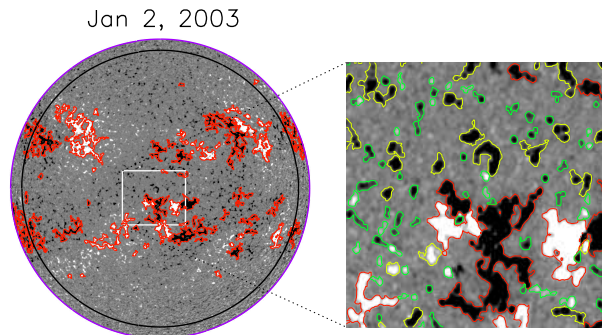
Figure 1. Left panel: The MDI 5-minute full-disk magnetogram. The active regions are contoured by red line. The black circle displays the location $\alpha=60°$. The gray scale saturates at ± 50 Mxcm^{-2}. Right panel: enlarged image for the windows framed in the MDI magnetogram, on which network elements falling in the flux ranges of $(2.9\text{-}32.0)\times 10^{18}$ Mx and $(4.3\text{-}38.0)\times 10^{19}$ Mx are outlines by green and yellow lines, respectively. Later, it will be demonstrated that the two types of network elements are anti-correlated and correlated with sunspot in the solar cycle.

genaar et al. 2003). More than 13 million network elements have been identified for the studied interval.

3. Results

3.1 Cyclic variations of network magnetic elements

We divide all the magnetic elements into 96 sub-groups according to the flux per element. The monthly number density of magnetic elements for each sub-group is calculated. The influences of the area changes of the quiet Sun and the changing distance between the Earth and the Sun have been removed. The correlation coefficients (i.e., the linear Pearson coefficients) between the cyclic variation of numbers of each sub-group network elements and sunspots are calculated and shown in the left panel of Fig. 2. From the small to large flux end in the flux spectrum, there appears a remarkable 3-fold correlation scheme between the network elements and the sunspots: basically no-correlation, anti-correlation and correlation. Either the anti-correlation or the correlation has been observed at very high confidence level. Between the anti-correlation and correlation, there is a narrow range of magnetic flux per element of $(3.2 - 4.3)\times 10^{19}$ Mx. Network elements falling in this flux range show a transition from anti-correlation to correlation with sunspot cycle.

For a further examination of cyclic behavior of network elements, we group all the network elements into 4 categories which show, respectively, no-correlation, anti-correlation, transition from anti-correlation to correlation, and correlation with sunspot
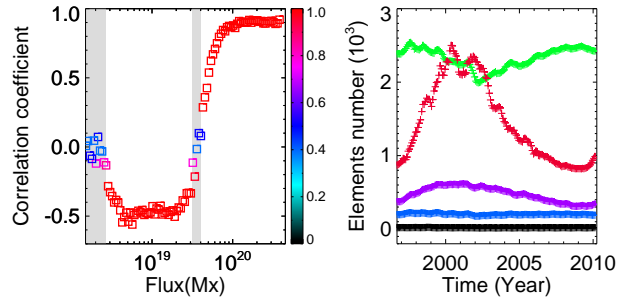
Figure 2. Left panel: correlation coefficients between the sunspot number and network element number of each of the 96 sub-group elements which are reconstructed according to the flux per element. The color bar represents the confidence level. Right panel: cyclic variations of network element number of 4 categories of network elements. The green '+' is referring anti-correlation elements, the purple '+' for the correlated elements, and the black and blue '+' for non-correlated elements and transitional elements from anti-correlation to correlation with the solar cycle. The red '+' shows the variation of sunspots.

cycle. The detailed cyclic variations of each category network elements are shown in the right panel of Fig. 2. In the flux range of $(1.5-2.9) \times 10^{18}$ Mx, network elements show randomly independent variation in the sunspot cycle. They occupy less than 0.6% of network elements. With the poor measurement sensitivity at the smallest flux range, the non-correlation component is likely to manifest some random noises in flux measurement. The correlated component elements have magnetic flux larger than 4.27×10^{19} Mx. They occupy approximately 15.7% of network elements. Approximate 77.2% of the magnetic elements, covering the flux range of $(2.9-32.0) \times 10^{18}$ Mx show anti-correlation with sunspots in the cycle. Their number changes are obviously anti-phased with the sunspot cycle. However, the cyclic minimum of this anti-correlation component is not exactly coincided with the maximum of the sunspot cycle.

3.2　The latitude distributions of the network elements

It is remarkable that the correlated magnetic elements follow exactly the sunspot butterfly diagram in the cycle except for that their latitude distribution is broader than that of sunspots (see the right panel of Fig. 3).

The anti-correlated elements also exhibit much broad latitude distribution than sunspots. The zone of their time-latitude distribution gradually shrinks toward the solar equator from 1996 to 2002, and concentrates on the narrowest latitude belt in the interval approximately from 2001 to 2002. Then, the distribution zone of anti-correlated magnetic elements gradually expands to higher latitude, and reaches the broadest latitude distribution in 2008 and 2009. The number of anti-correlated network elements
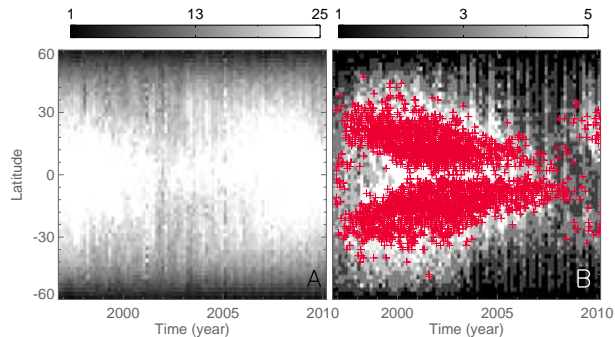
Figure 3. The time-latitude diagrams of network magnetic elements. Left: the time-latitude diagram for anti-correlated network elements. Right: for correlated network elements. The red symbols marks the sunspot distribution.

does show the latitudinal variation in the solar cycle, however, its latitude variation is clearly different from the butterfly diagram of sunspots.

4. Conclusions and discussion

Based on the unique database from MDI/SOHO observations, we have analyzed the cyclic variations of the solar network magnetic elements. With increasing magnetic flux per element the number of small-scale magnetic elements follows no-correlation, anti-correlation and correlation changes with sunspots. The anti-correlated component, covering the flux range of $(2.9 - 32.0) \times 10^{18}$ Mx, occupies 77.2% of total elements on the quiet Sun. Their time-latitude distribution is obviously different from the sunspot butterfly diagram in the sunspot cycle. However, the correlated network elements follow exactly the sunspot butterfly diagram but with a wider latitude distribution.

Mehltretter (1974) identified that the network bright points represented magnetic flux concentration. Golub et al. (1977) studied the magnetic properties of X-ray bright point, and found the average total flux associated with a typical X-ray bright point was 2.0×10^{19} Mx. This typical flux falls in the flux range of the anti-correlated component of network elements discovered by this study. Very recently, Sattarov et al. (2010) found the anti-correlation of the coronal bright points on the quiet Sun with sunspot in solar cycle 23. We tentatively suggest that the anti-correlated component of magnetic elements are responsible for the small-scale activity that is anti-phased with sunspot cycle.

Observationally, small-scale network elements come from several sources: fragmentation of active regions, flux emergence in the form of ephemeral regions, coalescence of intra-network flux, and products of dynamic interaction, e.g., flux cancellation, among different sources of magnetic flux.

From theoretical point of view, the magnetic elements at the smallest end of the flux spectrum manifest a local turbulent dynamo which operates in the near-photosphere and is suggested to be independent from the sunspot cycle. At the larger flux end, the magnetic elements are likely to be the debris of decayed sunspots. They naturally follow the sunspot cycle.

The majority of network magnetic elements are found to be anti-correlated with sunspots in the solar cycle. They are probably created by turbulent local dynamo which, however, must have been somehow modulated or controlled by the mean-field dynamo represented by sunspot magnetic fields. A thorough physical understanding on this is still not very much clear, though a few possibilities were proposed (see Jin et al. 2011; Jin & Wang 2011). Further observational and theoretical efforts are undertaken.

Acknowledgements

References

Davis J. M., 1983, Solar Phys., 88, 337
Davis J. M., Golub L., Krieger A. S., 1977, ApJ, 214, L141.
Golub L., Davis J. M., Krieger A. S. 1979, ApJ, 229, L145
Golub L., Krieger A. S., Harvey J. W., Vaiana G. S., 1977, Solar Phys., 53, 111
Hagenaar H. J., Schrijver C. J., Title A. M., 2003, ApJ, 584, 1107
Harvey K., 1985, Aust. J. Phys., 38, 875
Harvey K., Martin S. F., 1973, Solar Phys., 32, 389
Jin C., Wang J., Song Q., Zhao H., 2011, ApJ, 731, 37
Jin C., Wang J., 2011, ApJ(submitted)
Livingston W. C., Harvey J., 1975, BAAS, 7, 346
Mehltretter J. P., 1974, Solar Phys., 38, 43
Muller R., Roudier T., 1984, Solar Phys., 94, 33
Sattarov I., Pevtsov A. A., Karachik N. V., Sherdanov C. T., Tillaboev A. M., 2010, Solar Phys., 262, 321
Sheeley N. R. Jr., 1967, Solar Phys., 1, 171
Smithson R. C., 1975, BAAS, 7, 346
Trujillo Bueno J., Shchukina J. N., Asensio Ramos A., 2004, Nature, 430, 326
Zirin H., 1987, Solar Phys., 110, 101